URSI-RCRS 2024, ARIES/GEHU, Bhimtal, India, 22 - 25 October, 2024

Vital Sign Detection and Parameter Estimation using FMCW Radar

Abhijith S S[1], Swaroop Sahoo[1], Barghavi Parthiban[2], Karthik Ravindran[2], S. Gokhun Tanyer[2,3,4], Peter F. Driessen[4]
(1) Indian Institute of Technology, Palakkad, https://iitpkd.ac.in
(2) MulticoreWare Inc. San Jose, CA, USA
(3) INNOVTECH, Victoria BC, Canada
(4) University of Victoria, Victoria BC, Canada

Abstract

Millimeter-wave (mm-wave) radars, which use electromagnetic waves with wavelengths between 1 and 10 mm, can detect extremely small movements, down to a fraction of a millimeter. This capability makes them ideal for non-contact detection of human and pet vital signs. This paper introduces an algorithm designed to estimate both heart rate and breathing rate of individuals, whether seated inside a room or in cabin of a vehicle. The algorithm is implemented on in-phase signals from a frequency modulated continuous wave (FMCW) radar operating in the 58 – 63.5 GHz frequency range. The in-phase signal is used to analytically generate the quadrature signal using Hilbert transform. The impact of noise in the in-phase signal on the Hilbert transform is also investigated. A range scaling technique is implemented to compensate for propagation losses in target return signal increasing high probability of detection with a lower false alarm rate. Heart signal is obtained by bandpass filtering the phase signal extracted from the range bin that captures the information about chest and heart displacements. The performance of the algorithm is validated using both measured and simulated radar data. Radar data with signal to noise ratio (SNR) greater than -15dB are effective in accurately determining vital signs.

1. Introduction

The measurement of heart rate is crucial for assessing an individual's health and well-being. Continuous wave (CW) radar, impulse ultra-wideband (UWB) radar and FMCW radar are used for non-contact monitoring of vital signs [1]. FMCW radar offers superior resolution for both range and velocity detection compared to CW and UWB radars [2]. Millimeter-wave frequency signal can penetrate through ordinary clothing and reflect off the body surface, making them ideal for vital sign monitoring [3].

FMCW radar operating at 77 GHz is used to detect the vital sign of an individual lying down on a bed where target bins are selected after performing FFT on the phase samples and it is assumed that there are no random body motions [3]. Another FMCW radar operating at 80 GHz has been used to monitor the heart rate where it is assumed that the individual's location is known [4]. Furthermore, phase unwrapping and removal of DC resulting from phase modulation due to the chest vibration or from the leakage between transmit (Tx) antenna and receive (Rx) antenna are not done. The target bin is assumed to be the same across all the chirps [5]. Multiple-input multiple-output (MIMO) configuration along with maximal ratio combining (MRC) is used to enhance the SNR of the heart signal by optimally combining the vital sign signals acquired by different channels [6].

The proposed algorithm estimates the breathing and heart rates of individuals at rest within the radar field of view. The phase signal extracted from the range Fast Fourier Transform (FFT) output corresponding to the target bins carries information about chest and heart displacement, forming the basis for heart rate estimation. However, the estimation of heart rate poses several challenges, including the selection of target bins, enhancement of the SNR, and extraction of the heart signal from the phase signal. To address these challenges, this study proposes a comprehensive approach involving adaptive range bin selection, signal enhancement techniques, and signal extraction methods. Additionally, range scaling compensates for the propagation loss and ensures that individuals who are distant but within the radar's field of view are detected. Heart signal and breathing signal are extracted from the phase signal using bandpass filtering. The proposed algorithm was tested using measured radar data collected in various scenarios, including single person and two persons in a room. It was also tested with simulated radar data. Additionally, the impact of noise on the performance of the Hilbert transform is studied. The principles of using FMCW radar for heart and breathing rate estimation, along with the radar settings used for measurements, are detailed in Section 2. The initial signal processing chain which includes the application of Hilbert transform, range FFT, removal of static clutter and adaptive target bin selection algorithm is discussed in Section 3. The methods for estimating breathing rate and heart rate from the target bins are discussed in Section 4. The heart rate and breathing rate estimated from the radar measurements and the testing of the performance of the algorithm with simulated radar data are presented in the Subsections 4.1 and 4.2, respectively.

2. FMCW Radar Measurement

FMCW radar transmits linearly frequency-modulated sinusoidal wave, called chirp, and receives the reflected signal from the body of the subject. Therefore, it carries information about the heart and chest movements of the subject. The intermediate frequency (IF) signal is obtained by mixing the transmit signal and echo signal. The phase, $\boldsymbol{\phi}$, of the IF signal is related to the distance, $\boldsymbol{R_0}$, between the subject and radar, as well as the micro-movement, $\boldsymbol{x(t)}$, of the body surface given by the following equation [1].

$$\boldsymbol{\phi} = 4\boldsymbol{\pi}\frac{\left(\boldsymbol{R_0} + \boldsymbol{x(t)}\right)}{\boldsymbol{\lambda_{max}}} \tag{1}$$

As part of this research work, measurements have been performed using the Infineon BGT60TR13C FMCW radar according to the settings provided in Table 1. A collection of reflected signals corresponding to the transmitted chirps is referred to as frames. A total of 600 frames, each with 0.1 seconds duration, are collected over one minute. The radar range resolution is determined by the chirp bandwidth to be 10.7 cm, and the maximum range extends to 10.27 meters. The movements of the human thorax due to breathing and heart activity are minimal and the human body is located within a particular range bin unless random body motions or very large chest displacements occur.

Table 1: Radar settings used for taking the measurements

Radar parameters	Value
Start frequency of chirp (GHz)	60
End frequency of chirp (GHz)	61.4
Sampling frequency (KHz)	2000
Number of frames	600
Number of chirps per frame	128
Number of ADC samples per chirp	192
Frame duration (s)	0.1
Range resolution (cm)	10.7

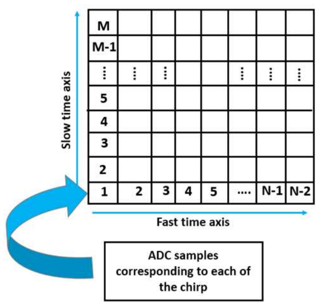

Figure 1. 2D radar data matrix

As an initial step in the analysis, a data matrix like the one depicted in Figure 1 is constructed. This involves storing the ADC samples for each chirp in a row, where multiple rows constitute a frame. The frame is a two-dimensional matrix where the horizontal axis of the data matrix is referred to as the fast time axis, while the vertical axis is termed the slow time axis. The time interval between two consecutive ADC samples in the same column should be such that the chest should not displace more than $\lambda_{max}/4$ within this time interval. This is necessary for the smooth operation of the phase unwrapping algorithm [3]. Also, the slow time sampling rate should be higher than twice the heart frequency. The maximum possible heart rate of human beings is usually 180 bpm (3 Hz) [7]. Therefore, the data matrix is constructed by selecting four chirps from each frame, ensuring that the time interval between consecutive samples along the slow time axis is 0.025 seconds.

3. Initial Signal Processing for Estimation Algorithm

The initial signal processing involves the generation of analytic quadrature signal from in-phase signal using the Hilbert Transform, performing FFT on the fast time axis of the data matrix to extract the target location. It is followed by range scaling to mitigate propagation loss, removal of static clutter, and selection of target bins using adaptive target bin selection technique. The block diagram illustrating the key steps in the heart and breathing rate estimation process is depicted in Figure 2. Further elaboration on the important steps is provided in the subsequent sections.

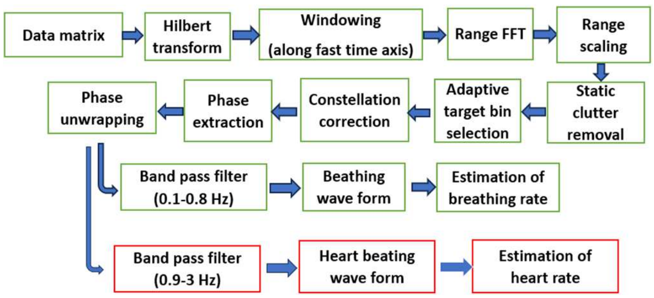

Figure 2. Signal processing chain for the estimation of breathing and heart rate

3.1. Hilbert Transform and Noise Analysis

The process mentioned in Section 2 requires the use of complex signal. But the ADC samples obtained from the Infineon radar, are real-valued. However, a complex analytical signal can be generated using Hilbert transform. By applying the Hilbert transform to the real signal, a 90° phase-shifted imaginary part of the signal can be constructed. Suppose f(t) is a real signal, then the Hilbert transform of f(t), denoted as H(f(t)), can be obtained by convolving f(t) with 1/πt [8]. The complex signal $f_c(t)$ can be represented as,

$$f_c(t) = f(t) + j\,H(f(t)) \tag{2}$$

It has to be noted that the real signal may not have a very good SNR (greater than 25 dB) [9]. Therefore, the performance of the Hilbert transform can be affected by the noise present in the signal. To analyze the impact of noise (noisy real signal) on the Hilbert transform, a set of real values (I) from a particular column of the data matrix is selected. Thereafter, the quadrature phase values (Q) are determined by applying the Hilbert transform. The assumption here is that the real valued signal used for calculating the Q are devoid of noise. The next step involves adding Gaussian noise with a mean of zero to the in-phase values and calculation of quadrature phase values by applying Hilbert transform and the corresponding SNR. This process is repeated 24,000 times for each SNR value by regenerating the noise. The Q values estimated after adding noise to the I values are compared with the noise-free Q values, and the mean square error (MSE), root mean square error (RMSE), and mean absolute error (MAE) are calculated. The variation of MSE, RMSE, and MAE are shown in the Figure 3. The results indicate that the noisy real signal impacts the Hilbert transform output. The errors of the Hilbert transform output changes with SNR. It can be observed that as the SNR increases, the errors reduce. Primarily, errors are approximately equal to zero at an SNR greater than 0 dB.

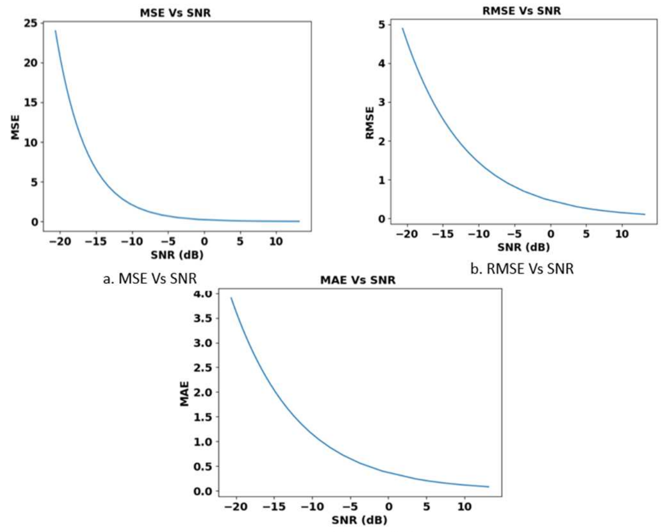

a. MSE Vs SNR b. RMSE Vs SNR c. MAE Vs SNR

Figure 3. Variation of MSE, RMSE and MAE of Q values with SNR

3.2. Static Clutter Removal Technique

As per the initial signal processing, after FFT implementation and range scaling, the range-slow time map is generated. The range slow-time map is shown in Figure 4. Range slow time map It can be observed that the target location is not clear and reflections from stationary objects (clutter) are obscuring the target location.

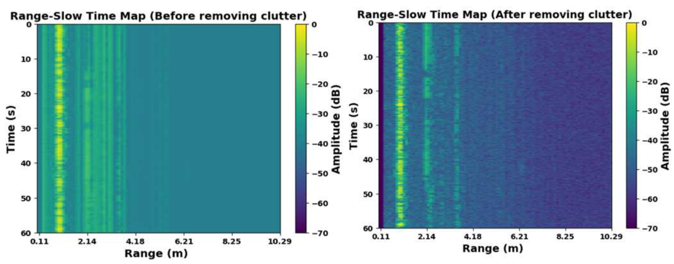

(a) Before removing clutter (b) After removing clutter

Figure 4. Range slow time map

Mitigating the effects of clutter can improve the accuracy of target detection, estimation of breathing and heart rates. To mitigate the effects of clutter, mean of FFT output (range-slow time map) corresponding to each of the range bins is computed and subtracted from the FFT outputs in the respective range bins [1]. After clutter removal the target location is clear as per Figure 4 (b).

3.3. Target Detection and Bin Selection

Random body motion and large chest displacement can result in variations of target bins for each chirp. Therefore, the adaptive target bin selection algorithm chooses the range bin with maximum energy in which the information corresponding to heart rate is present. This is accomplished as follows:

- The two-dimensional range FFT matrix is divided into several units (U_i) with each unit containing 'K' number of chirps.
- For U_{i-1}, best bin is selected based on the peak of summation of FFT output of K chirps. Summation is performed along the slow time axis.
- Suppose the best bin selected for the unit U_{i-1} is R_j, then the best bin corresponding to the unit U_i is selected in the following way.
    - The sum of the magnitudes of the FFT outputs (along the slow time) is separately found for each of the range bins R_j and its adjacent range bins R_{j-1} and R_{j+1}.
    - The range bin with highest summation value is selected as the best bin for all the chirps of the unit U_i. This process is repeated for all units.

4. Estimation of the Vital Signs

Phase is extracted from the best range bins using the $\arctan(y/x)$ function, where x and y are the real and the imaginary parts of the FFT output after constellation correction. Constellation correction is performed to remove the DC part present in the real and imaginary part [3]. After that, phase extraction is conducted, followed by phase unwrapping [5]. The breathing frequency of humans typically falls in the range of 0.1 – 0.8 Hz. An infinite impulse response (IIR) filter is used as a band pass filter to extract the breathing waveform from the phase signal. The breathing rate is determined by tracking the frequency corresponding to the maximum peak in the frequency spectrum. The heart beating frequency of humans typically falls in the range of 0.9 –3 Hz. The phase signal is bandpass filtered with suitable lower and upper cutoff frequencies to estimate the heart signal.

4.1. Vital Signs from Radar Measurements

Measurements have been taken inside a room with single person and two persons present in the field of view of the radar. The heart rate and breathing rate estimated for these cases are provided in Table 2. The heart rates were also measured by smart watch worn by the participants and are presented in the Table 2. Additionally, errors associated with heart rate values are presented as Mean Absolute Error (MAE) and Mean Absolute Percentage Error (MAPE) in Table 2. It can be observed that the maximum MAE is 9 bpm and maximum MAPE is 12 %.

Table 2. Estimated heart rate and breathing rate values

Cases	Heart rate measured by smart watch (bpm)	Breathing rate (bpm)	Estimated heart rate (bpm)	MAE (bpm)	MAPE (%)
SINGLE PERSON					
Normal breathing	72	14	65	7.5	10.42
Fast breathing	103	61	101	2.5	2.43
Deep breathing	67	10	66	3	4.48
TWO PERSONS					
Normal breathing Person 1	65	16	66	3	4.62
Normal breathing Person 2	75	19	74	9	12

4.2. Algorithm Performance Testing with Simulated Radar Data

Radar data set has been created for testing the performance of the estimation algorithm. The radar data is created assuming heart frequency to be 1 Hz and radar is transmitting sinusoidal signal. To simulate the noise of the radar and environment, Gaussian noise is created and added to the simulated radar data. The Gaussian noise is such that the SNR range is -60 to 20 dB with an interval of 1 dB. The results are presented in Figure 5. It can be observed that the estimated heart rate has a high amount of variation from SNR range of -60 to -17 dB. As the SNR improves, the estimated heart rate becomes more accurate.

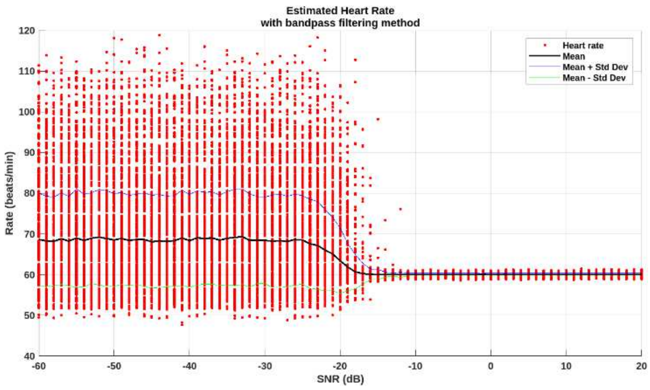

Figure 5: Estimated heart rate versus the SNR. (red) estimated heart rates, (black) mean, (blue and green) one standard deviation above and below the mean

5. Conclusion

An algorithm for heart and breathing rates estimation has been analyzed. This is observed to be accurate even in the case of sensing heart rate of multiple persons. Adaptive target bin selection technique is effective in selecting the best bins containing information about heart and chest displacement. It is shown that successful estimating of heart rate (HR) and breathing rate (BR) estimations within 0.03 Hz error (2 bpm) is possible for SNRs above –17 dB. The error in the Hilbert transform computed Q values is approximately zero above an SNR of 0 dB, and interestingly the algorithm is found to be effective also in the range between –17 dB and 0 dB. One disadvantage of the algorithm is that multi-target separability is not possible when individuals are located in the same range bin. Potential areas for further research and algorithm optimization include defining additional performance metrics; HR and BR estimation in the shortest time, minimization of computations, and simultaneous detection of slowly moving targets.

References

1. M. Zhou, Y. Liu, S. Wu, C. Wang, Z. Chen and H. Li, "A Novel Scheme of High-Precision Heart Rate Detection With a mm-Wave FMCW Radar," in *IEEE Access*, vol. 11, pp. 85118-85136, 2023, doi: 10.1109/ACCESS.2023.3303335.
2. Wang, Y.; Wang, W.; Zhou, M.; Ren, A.; Tian, Z, "Remote Monitoring of Human Vital Signs Based on 77-GHz mm-Wave FMCW Radar," *Sensors* 2020, 20, 2999. https://doi.org/10.3390/s20102999.
3. M. Alizadeh, G. Shaker, J. C. M. D. Almeida, P. P. Morita and S. Safavi-Naeini, "Remote Monitoring of Human Vital Signs Using mm-Wave FMCW Radar," in *IEEE Access*, vol. 7, pp. 54958-54968, 2019, doi: 10.1109/ACCESS.2019.2912956.
4. S. Wang *et al*., "A novel ultra-wideband 80 GHz FMCW radar system for contactless monitoring of vital signs," *2015 37th Annual International Conference of the IEEE Engineering in Medicine and Biology Society (EMBC)*, Milan, Italy, 2015, pp. 4978-4981, doi: 10.1109/EMBC.2015.7319509.
5. K. Liu, C. Ding and Y. Zhang, "A Coarse-to-Fine Robust Estimation of FMCW Radar Signal for Vital Sign Detection," *2020 IEEE Radar Conference (RadarConf20)*, Florence, Italy, 2020, pp. 1-6, doi: 10.1109/RadarConf2043947.2020.9266599.
6. T. K. V. Dai *et al*., "Enhancement of Remote Vital Sign Monitoring Detection Accuracy Using Multiple-Input Multiple-Output 77 GHz FMCW Radar," in *IEEE Journal of Electromagnetics, RF and Microwaves in Medicine and Biology*, vol. 6, no. 1, pp. 111-122, March 2022, doi: 10.1109/JERM.2021.3082807.
7. Fernhall B, McCubbin JA, Pitetti KH, Rintala P, Rimmer JH, Millar AL, De Silva A. Prediction of maximal heart rate in individuals with mental retardation. *Med Sci Sports Exerc.* 2001 Oct;33(10):1655-60. doi: 10.1097/00005768-200110000-00007. PMID: 11581548.
8. A. I. Zayed, "Hilbert transform associated with the fractional Fourier transform," in *IEEE Signal Processing Letters*, vol. 5, no. 8, pp. 206-208, Aug. 1998, doi: 10.1109/97.704973.
9. S. Ayhan, S. Scherr, A. Bhutani, B. Fischbach, M. Pauli and T. Zwick, "Impact of Frequency Ramp Nonlinearity, Phase Noise, and SNR on FMCW Radar Accuracy," in *IEEE Transactions on Microwave Theory and Techniques*, vol. 64, no. 10, pp. 3290-3301, Oct. 2016, doi: 10.1109/TMTT.2016.2599165.